

Calculated effect of anorthite component on the crystallization paths of H₂O-undersaturated haplogranitic melts

HANNA NEKVASIL*

Geology Department, Arizona State University, Tempe, Arizona 85287, U.S.A.

ABSTRACT

Equilibrium crystallization paths were calculated for several compositions in the “granite” system (i.e., the system Ab-An-Or-Qz-H₂O) using the revised quasi-crystalline model in order to systematically evaluate the effect of anorthite melt component (An) on H₂O-undersaturated crystallization paths. When H₂O is an independent compositional variable, the four-phase (alkali feldspar + quartz + melt + “vapor”) H₂O-saturated haplogranite cotectic becomes a limiting curve of the three-phase (alkali feldspar + quartz + melt) cotectic surface(s) in the haplogranite system, and the H₂O-saturated five-phase curve becomes a limiting curve of the four-phase surface in the plagioclase-bearing “granite” system. For H₂O-undersaturated compositions, the presence of these surfaces results in Qz enrichment of the melt during cotectic crystallization of alkali feldspar and quartz from haplogranitic melts and during coprecipitation of alkali feldspar, quartz, and plagioclase in “granitic” melts. Inasmuch as the four-phase surface (plagioclase + alkali feldspar + quartz + melt) exists at very low An contents, “granitic” crystallization paths are characterized by major early depletion of An from the melt but only slight later depletion during the coprecipitation of the three crystalline phases. Melts produced by differentiation or partial melting along the four-phase surface lie (in projection into the haplogranite system) toward the Or-Qz sideline relative to the haplogranite minima. As the An content of the bulk composition increases, the entire crystallization path shifts away from the Ab-Qz sideline. The solidus temperatures, however, vary only slightly with bulk An content because of the very small temperature dependence of the five-phase H₂O-isoactivity curves. With increasing total pressure, the compositional variability of the melt along the crystallization paths increases. The extent of crystallization within the crystallization temperature interval (i.e., between the liquidus and the solidus) is heavily weighted toward the late stages of crystallization. High bulk H₂O contents strongly enhance this effect (e.g., as little as 5% crystallization may take place during the first 50% of the crystallization temperature interval in some H₂O-rich “granitic” magmas).

INTRODUCTION

The most directly accessible information regarding the melting and crystallization history of an igneous body is that provided by the textural and chemical characteristics of the body itself. Arriving at a unique interpretation of such characteristics is problematic, however, because the textures and composition of the body represent the end products of numerous possible petrogenetic pathways. Understanding the history of the body, therefore, requires that investigative efforts go beyond the present features of the body and toward evaluation of the general effects of geologically relevant variables such as pressure, temperature, and volatile content on pathways of development of magmatic bodies. The results of such efforts can be used in turn to interpret the information obtained from a specific igneous body on a rigorous basis and, it is hoped,

to permit the reconstruction of the processes that were involved in its development. The following discussion will concentrate on one very important aspect in the development of the mineralogical characteristics of felsic bodies—the changes in melt and crystal compositions and proportions that occur during the crystallization of felsic magmas. The predicted effects of pressure, H₂O content (X_w), activity of H₂O (a_w), and composition on these changes will be evaluated by investigating the trends of crystallization paths for several compositions lying in the “granite” system (i.e., the system Ab-An-Or-Qz-H₂O).

The revised “quasi-crystalline” model of silicate melts (Burnham, 1981; Nekvasil, 1986; Burnham and Nekvasil, 1986; Nekvasil and Burnham, 1987) was used as the basis for calculations of crystallization paths. The methods used in these calculations are discussed by Nekvasil (1988). All of the compositions selected for this study lie within the “granite” system (i.e., the system Ab-Or-An-Qz-H₂O) and represent approximations of the compositions of natural felsic rocks with normative Ab + Or +

* Present address: Department of Earth and Space Sciences, State University of New York at Stony Brook, Stony Brook, New York 11794-2100, U.S.A.

$Qz + An \geq 90\%$. The results of this investigation will be discussed first for the haplogranite system (i.e., the system Ab-Or-Qz-H₂O) and then for similar compositions lying in the "granite" system in order to permit the direct comparison of crystallization paths in the plagioclase-free system with those of the plagioclase-bearing system.

THE HAPLOGRANITE SYSTEM REVISITED

The haplogranite system has been used extensively as a model system for the crystallization behavior of felsic magmas since the work of Tuttle and Bowen (1958) and Luth et al. (1964). In reflection of the azeotropic relationship in the bounding subsystem Ab-Or-H₂O, the haplogranite system at low pressures contains a thermal minimum on the alkali feldspar + quartz + liquid + vapor cotectic curve (Tuttle and Bowen, 1958). At higher P_{H_2O} , this thermal minimum becomes a ternary eutectic (Luth et al., 1964) as the solidus intersects the alkali feldspar solvus. Both the position of the minimum and the ternary eutectic in the haplogranite system are of great importance in the "granite" system because they represent the limiting position of the curve delineating coexistence of plagioclase, alkali feldspar, quartz, melt, and vapor (assumed to be pure H₂O) (i.e., the five-phase curve) as the An content of the melt approaches zero. Any shift of the haplogranite minimum (or eutectic) composition with pressure and H₂O content will be reflected by a similar shift in the five-phase curve, thereby making an investigation of the former an indirect investigation of the latter.

The experimental determinations of the haplogranite thermal minima of Tuttle and Bowen (1958) and of Luth et al. (1964) were conducted under H₂O-saturated conditions. Their results, therefore, reflect the combined effects of increasing pressure and H₂O content. Nekvasil and Burnham (1987), using the revised "quasi-crystalline" model (Burnham and Nekvasil, 1986), calculated the phase relations in the haplogranite system for H₂O-undersaturated conditions at several pressures. Their work indicates that with increasing pressure at constant H₂O content, the quartz + liquid field expands and the quartz + alkali feldspar + liquid cotectic (as well as the minimum or eutectic) shifts to lower Qz contents. In contrast, the quartz + liquid field contracts with increasing H₂O content at constant total pressure, and the composition of the minimum shifts toward more Qz-rich compositions. For H₂O-saturated conditions, the quartz + liquid field expands with increasing P_{H_2O} , albeit to a slighter extent than under H₂O-undersaturated conditions (in agreement with the experiments of Tuttle and Bowen, 1958, and Luth et al., 1964). This result can be attributed to the opposing effects of the simultaneous increase in pressure and H₂O that occur upon increasing P_{H_2O} .

It is now widely believed that most deep-seated felsic magmas attain H₂O saturation only during the late stages of their crystallization history. This implies that the melt will remain H₂O-undersaturated over a large portion of the crystallization temperature interval. Therefore, in order for the haplogranite system to be a more useful model

system, phase relations must be known for variable H₂O contents at constant total pressure; that is, H₂O must be considered an independent compositional variable. Luth (1969) recognized this need and attempted to evaluate the effect of H₂O content on the bounding subsystems (i.e., the systems Ab-Qz-H₂O and Or-Qz-H₂O), as well as on the haplogranite quartz + feldspar cotectic, by determining anhydrous phase relations at pressures of 8 to 20 kbar. These anhydrous relations, when combined with H₂O-saturated data, permitted the evaluation of the general trends in the variation of eutectic and cotectic positions with H₂O content. For the system Or-Qz-H₂O at 10-kbar total pressure, Luth (1969) found that an increase in H₂O content induced a marked contraction of the quartz + liquid field and concomitant shift of the eutectic to higher Qz contents. For the system Ab-Or-H₂O, however, he determined that a similar increase in H₂O resulted in essentially no change in the Qz content of the eutectic. On the basis of these results he speculated that at 5-kbar total pressure, the quartz + liquid (+ vapor) field would expand with increasing H₂O content, thereby shifting the eutectic composition in the system Ab-Qz-H₂O to lower Qz contents. At 1 kbar, however, he speculated that there would be little change in the extent of the quartz + liquid field. It is difficult to understand the basis for the prediction of such irregular behavior in the Ab-Qz-H₂O system. Inasmuch as data were obtained only at pressures of 10 kbar and above and in view of the likelihood of encountering equilibrium problems in determining the position of the anhydrous eutectic at such high pressures and short run times, it is unreasonable to conclude that a marked difference in eutectic behavior with variable H₂O content should be expected between the systems Or-Qz-H₂O and Ab-Qz-H₂O. Instead, from the larger $\Delta H_{\text{fus}}^{\text{albite}}$ relative to that for Si₄O₈ (see discussion of Nekvasil and Burnham, 1987) and the approximations that H₂O mixes similarly in albite and sanidine melts (Burnham, 1975; Silver and Stolper, 1985) and that mixing of the anhydrous aluminosilicate components and Si₄O₈ is ideal (Burnham, 1981; Hervig and Navrotsky, 1984), it is more reasonable to expect that upon increasing H₂O content at constant total pressure, the quartz field will contract in both systems.

Steiner et al. (1975) supplemented the work of Luth (1969) by investigating the phase relations in the haplogranite system at 4-kbar total pressure as a function of H₂O content. They concluded that their results support the speculations of Luth (1969) regarding the differences in direction of shift of the eutectic in the system Or-Qz-H₂O relative to that in the system Ab-Qz-H₂O with increasing H₂O content. However, from the compositional limits indicated by their data, it need not be concluded that the Qz content of the eutectic decreases with increasing H₂O content; instead the Qz content could even be considered to increase slightly.

The calculated effects of variable a_w and pressure on the positions of the haplogranite cotectics and thermal minima are shown in Figure 1. The calculation method used in obtaining the cotectics is as described in Nekvasil

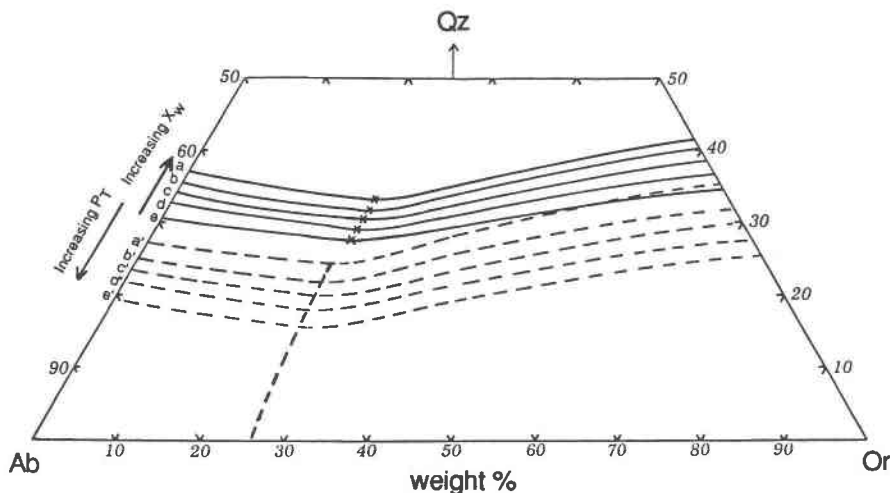


Fig. 1. Calculated cotectic surfaces of the system Ab-Or-Qz-H₂O at 2 kbar (solid curves) and 10 kbar (dashed curves) projected onto the anhydrous haplogranite base as two sets of cotectic H₂O isoactivity curves. The positions of the thermal minima along the 2-kbar isoactivity curves are indicated by converging arrowheads. Curves a-e and a'-e' refer to the a_w (activity of H₂O in the melt), which varies from 1.0 to 0.20 in increments of 0.20 (the highest a_w being closest to the Qz apex). The temperatures at the intersections of these isoactivity curves with the 10 wt% Or isopleth are 748, 765, 801, 841, and 891 °C (in order of decreasing a_w) for 2 kbar and 644, 710, 776, 846, and 928 °C at 10 kbar. The temperatures at the intersections of the isoactivity curves with the 50 wt% Or isopleth are 770, 785, 817, 854, and 875 °C at 2 kbar and 689, 748, 809, 873, and 950 °C at 10 kbar. Arrows indicate the directions of increasing X_w (mole fraction of H₂O in the melt) and P (total pressure).

and Burnham (1987) for the calculation of phase equilibria using the revised quasi-crystalline model. The activities of H₂O referred to in this article are those calculated with the albite-H₂O model (Burnham, 1975), as discussed in Burnham and Nekvasil (1986). Figure 1 shows the calculated alkali feldspar + quartz cotectics at 2 and 10 kbar for $a_w = 0.2, 0.4, 0.6, 0.8,$ and 1.0. It can be readily seen that the calculated effect of increasing a_w in the melt at constant total pressure (and therefore increasing H₂O content, albeit nonlinearly) is the contraction of the quartz + liquid field. As discussed in Nekvasil and Burnham (1987), this differential contraction is a consequence of the smaller ΔH_{fus} of Si₄O₈ relative to that of the feldspar

components. The extent of this contraction increases with pressure for a given Δa_w in response to the increase in $X_{w,\text{sat}}$ with pressure. The effect of increasing pressure at constant a_w , on the other hand, is the expansion of the quartz + liquid field. These cotectic H₂O isoactivity curves map out the cotectic surface in the system Ab-Or-Qz-H₂O.

A listing of the calculated haplogranite thermal minima at 2, 5, and 10 kbar and variable a_w is given in Table 1. The Or content of the haplogranite minima (and eutectics) remains fairly constant (at approximately 24 wt%) with increasing a_w as well as increasing total pressure. The Qz contents of the minimum melts, however, show systematic variations; these variations with temperature and a_w for 2, 5, and 10 kbar are shown in Figure 2. With increasing total pressure, the temperature change per unit change in a_w increases as a result of the increased solubility of H₂O at higher pressures. This effect is also reflected by an increased shift in Qz content at higher pressures. At low H₂O activities, lowering of the total pressure results in a decrease of the minimum temperature; at higher H₂O activities, it results in an increase. The isoactivity tie lines in Figure 2 indicate that for any interval of pressure change, an a_w exists such that the initial and final minimum temperatures will remain the same. At very low pressures (e.g., 0.5 kbar) the minimum temperatures for each a_w will increase with decreasing pressure.

For H₂O-saturated haplogranitic melts, the crystallization paths of melts within the haplogranite system are simple. The melt moves away from the instantaneous solid-phase composition until a cotectic is intersected. At this point the second phase begins to coprecipitate with

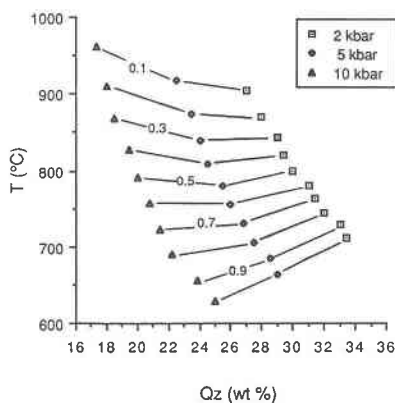


Fig. 2. Variation in the Qz content and temperature of the haplogranite minima with pressure and a_w at 2-, 5-, and 10-kbar total pressure. The numbers indicated along the tie lines refer to a_w .

the first, and the melt slides toward the solidus. Such a crystallization path implies that a series of daughter melts could be produced that would be initially depleted or enriched in Qz depending upon the identity of the liquid phase. However, upon the onset of coprecipitation of the two crystalline phases, alkali feldspar and quartz, the melt will become slightly depleted in Qz as it shifts toward the solidus, irrespective of the identity of the liquid phase. The crystallization-path trends exhibited by H₂O-saturated melts will also characterize the crystallization trends of H₂O-undersaturated melts that remain buffered with respect to H₂O throughout their crystallization history (a situation unlikely in nature but becoming increasingly popular for laboratory conditions).

Crystallization paths of unbuffered haplogranitic melts that are H₂O undersaturated will differ from those crystallizing under H₂O-buffered conditions in accordance with the nature of the cotectic surface. Taking as an example the composition Qz₃₇Or₃₃Ab₃₀ (HG-1) at 2 kbar with bulk H₂O content of ~1.7 wt% (i.e., 20 mol%), the calculated closed-system equilibrium crystallization path is shown in Figure 3a by means of a projection from the H₂O apex of the system Ab-Or-Qz-H₂O onto the anhydrous haplogranite base. Quartz is the liquidus phase under the given conditions, and its precipitation will deplete the melt in Qz, driving it directly away from the Qz apex. At 879 °C, however, the melt path intersects the cotectic surface at the isoactivity cotectic curve for which $a_w = 0.23$ ($X_w = 0.22$; ~1.9 wt% H₂O), and alkali feldspar of Or₇₂ composition begins to coprecipitate with quartz. Instead of following the isoactivity curve to lower Or and Qz contents upon further crystallization (as would be the case if the a_w were buffered), the melt path cuts across the cotectic surface, that is, across the projected set of H₂O isoactivity cotectic curves. Consequently, the melt now becomes enriched in Qz (in addition to Ab) until the H₂O-saturated cotectic is reached. Upon further crystallization, the melt will exsolve H₂O and slide down this cotectic to lower Qz and Or contents until the solidus is reached. For the composition HG-1, the solidus is reached before the melt attains the haplogranite minimum composition, and because the bulk H₂O content is low enough, the H₂O-saturated cotectic is not reached until very close to the solidus. If instead, the bulk H₂O content were higher, the H₂O-saturated cotectic would be intersected much before the solidus is reached. The main difference between the crystallization path of a haplogranitic melt crystallizing under H₂O-unbuffered conditions relative to one crystallizing under H₂O-buffered conditions is, therefore, the enrichment of the melt in Qz that begins at the onset of coprecipitation of both crystalline phases and continues until the H₂O-saturated cotectic is reached.

The crystallization path for the composition HG-2 (Qz₂₆Or₄₀Ab₃₄) at 2 kbar and 1.7 wt% H₂O is plotted for comparison in Figure 3a. This composition has alkali feldspar of Or₇₄ composition on the liquidus at 2-kbar and quartz on the liquidus at 5-kbar total pressure. At 2 kbar, the precipitation of alkali feldspar alone continues

TABLE 1. Calculated haplogranite minima compositions along the cotectic H₂O isoactivity curves of Figure 1

T (°C)	H ₂ O		Or (wt%)	Ab (wt%)	Qz (wt%)
	a_w	X_w (wt%)			
P = 2.0 kbar					
904	0.10	0.15	1.2	23.9	49.1
870	0.20	0.21	1.8	23.9	48.1
844	0.30	0.26	2.4	24.0	47.0
820	0.40	0.30	2.9	24.0	46.5
800	0.50	0.33	3.4	24.0	46.0
780	0.60	0.36	3.8	24.0	45.0
762	0.70	0.39	4.3	24.0	44.5
744	0.80	0.42	4.8	24.0	44.0
728	0.90	0.45	5.3	24.0	43.0
711	1.00	0.47	5.8	24.0	42.5
P = 5.0 kbar					
917	0.10	0.19	1.5	24.0	53.5
874	0.20	0.27	2.4	24.0	52.5
839	0.30	0.32	3.1	24.0	52.0
808	0.40	0.37	3.9	24.0	51.5
780	0.50	0.41	4.6	24.0	50.5
755	0.60	0.47	5.3	23.7	50.1
730	0.70	0.49	6.1	23.5	49.7
706	0.80	0.51	6.8	23.0	49.5
685	0.90	0.55	7.7	23.0	48.5
663	1.00	0.57	8.5	23.0	48.0
P = 10.0 kbar					
962	0.10	0.23	2.0	24.0	58.7
911	0.20	0.32	3.1	24.0	58.0
867	0.30	0.39	4.2	24.0	57.5
828	0.40	0.46	5.4	24.0	56.6
791	0.50	0.51	6.5	24.0	56.0
757	0.60	0.55	7.7	24.0	55.2
725	0.70	0.59	8.8	24.0	54.5
689	0.80	0.62	10.1	23.5	54.3
655	0.90	0.70	12.8	23.0	53.2
628	1.00	0.71	14.6	23.0	52.0

for only a very short segment of the crystallization interval; quartz appears after only 6 mol% of the system has crystallized. As was the case for HG-1 under H₂O-undersaturated and unbuffered conditions, the melt will continue to be enriched in Qz until the H₂O-saturated cotectic is reached. Continued crystallization will reduce the Qz content of the melt as this cotectic is followed. As was determined to be the case for HG-1 (for ~1.7 wt% H₂O), the solidus of HG-2 lies close to the minimum but not exactly at the minimum.

Figure 3b shows the crystallization path of HG-1 at 5 kbar for the same bulk H₂O content as at 2 kbar (~1.7 wt%). Quartz begins to precipitate as the liquidus phase at a higher temperature than is the case at 2 kbar (~1055 °C). The increase in quartz stability with pressure (as indicated by the shift of the cotectic surface to lower Qz contents as shown in Figure 1) implies that crystallization must proceed further before alkali feldspar is stabilized. For the composition HG-1, the fraction of liquid remaining at the onset of precipitation of alkali feldspar decreases from 91 to 86 mol% as the total pressure is increased from 2 to 5 kbar. Alkali feldspar of Or₇₆ composition begins to coprecipitate with quartz at ~910 °C when the $a_w = 0.15$ ($X_w = 0.232$, wt% H₂O = 2.0). The solidus does not lie at the ternary eutectic for this bulk composition; therefore, two feldspar phases will not be stabilized at any temperature along the crystallization

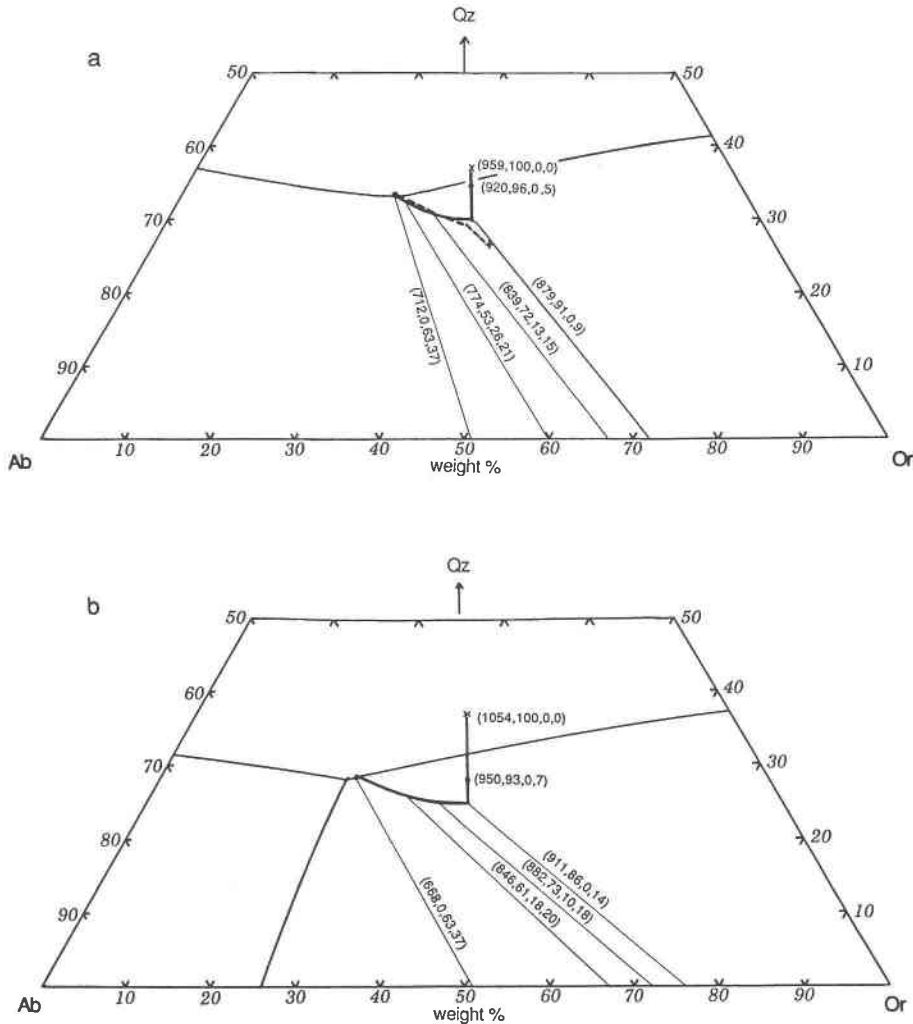


Fig. 3. Calculated crystallization paths for HG-1 (bulk composition: $Qz_{37}Or_{33}Ab_{30}$; bulk H_2O content: 1.7 wt% as indicated by the \times) at (a) 2-kbar and (b) 5-kbar total pressure (shown by the solid curve) and for HG-2 (bulk composition: $Qz_{26}Or_{40}Ab_{34}$; bulk H_2O content: 1.7 wt% as indicated by the $+$) at 2 kbar [shown by the dashed curve in a]. Tie lines connect coexisting feldspar and melt compositions. The temperature ($^{\circ}C$) and the proportions of melt, alkali feldspar, and quartz (mol%) are shown in parentheses along the appropriate tie lines for HG-1. For comparison, the H_2O -saturated cotectic at 2 kbar is also shown.

path, and the mode will show only an Or-rich feldspar and quartz.

For HG-1 at 2-kbar total pressure, Figure 4a shows the variation in modal percentages (X_i on a mole fraction basis) of crystalline and melt phases relative to their abundances at the solidus ($X_{i, \text{solidus}}$) as a function of the fraction of the total crystallization temperature interval attained [i.e., $(T_{\text{liquidus}} - T)/(T_{\text{liquidus}} - T_{\text{solidus}})$]. The variation in degree of crystallinity with $(T_{\text{liquidus}} - T)/(T_{\text{liquidus}} - T_{\text{solidus}})$ is shown by the variation of the total fraction of solids (F_S , i.e., $X_{\text{quartz}} + X_{\text{alkali feldspar}}$, relative to their proportions at the solidus) and melt (F_L). (F_L is calculated relative to its proportion at the liquidus.) The variation of these two parameters are not complementary, however, because F_L varies from 1 to 0 while F_S varies from 0 to 1 - X_w [i.e., at the solidus $F_L = 0$ but X_w ("vapor") + $F_S = 1$]. The characteristics of the variation in F_L are

dependent on the identity of the crystalline phase or phases precipitating. During the early precipitation of quartz, the fraction of liquid changes slowly. Once alkali feldspar begins to coprecipitate with quartz, however, the fraction of liquid decreases more rapidly (as the melt path cuts across the H_2O -undersaturated cotectic surface) until the H_2O -saturated cotectic is reached. The very slight temperature variation along the H_2O -saturated cotectic results in a large extent of crystallization within a very small temperature interval near the solidus. Both quartz and alkali feldspar precipitate almost linearly over the crystallization temperature interval although the extent of change with temperature interval diminishes slightly at higher F_S (until H_2O saturation is achieved). As is expected behavior along the cotectic, the onset of precipitation of alkali feldspar results in an increase in the amount of quartz precipitated per unit change in temperature ow-

ing to the counteracting effects of Qz depletion in the melt due to quartz precipitation and Qz enrichment in the melt due to feldspar precipitation. For the composition HG-1, approximately 90% of the crystallization occurs during the coprecipitation of alkali feldspar and quartz. Therefore, any daughter melts produced by a reasonable degree of differentiation (>10%) of a melt similar in composition to HG-1 would have both quartz and alkali feldspar on the liquidus.

At 5 kbar (Fig. 4b), the variations in modal assemblage take on more exaggerated characteristics. When alkali feldspar begins to precipitate with quartz, the fraction of liquid drops markedly, but this decrease is moderated at lower temperatures. Inasmuch as the initial H₂O content of the melt is still 1.7 wt%, the activity of H₂O is much lower at 5 kbar than at 2 kbar. Therefore, a greater degree of crystallization is required before H₂O saturation is attained (i.e., F_L will be lower) and the H₂O saturation temperature will be very close to the solidus temperature.

Compositions HG-1 and HG-2 were chosen as representative of felsic compositions with normative Ab + Or + Qz > 0.80. This decision was based on the frequency-of-occurrence contours from the compilations of projected natural felsic compositions presented in Washington's tables (1917) as shown by Tuttle and Bowen (1958) and James and Hamilton (1969) and replicated in Figure 5. From the very limited variability of natural projected compositions, it is reasonable to conclude that the compositions lying within the field of the highest-density contour will follow crystallization paths similar to HG-1 or HG-2. Consequently, for the majority of such compositions, most of the crystallization will occur during the coprecipitation of alkali feldspar and quartz.

The major problem in using the crystallization path characteristics of haplogranitic compositions to infer the characteristics of the crystallization paths of compositionally more complex granites is the implicit assumption that the influence of "other" components on the crystallization path is minor. For most felsic rocks, the "other" component perceived as being most important is An. Even a small amount of An in a felsic melt is likely to produce an additional feldspar phase (plagioclase) at low P_{H_2O} and to increase the stability range of plagioclase at high P_{H_2O} . In the section below, discussion will focus on the effect of adding An to melts in the haplogranite system in order to assess, by comparison, its effect on the crystallization paths of compositions with normative Ab + Or + Qz + An \geq 80%.

THE "GRANITE" SYSTEM

Crystallization paths followed by Ca-bearing felsic melts low in MgO + FeO reflect the phase relations in the "granite" tetrahedron (i.e., the system Ab-Or-An-Qz). The general configuration of the cotectic surfaces within the tetrahedron has been described by Carmichael (1963) and by subsequent workers (e.g., James and Hamilton, 1969; Winkler and Lindemann, 1972; Nekvasil and Burnham, 1987) as more data became available. Contained within

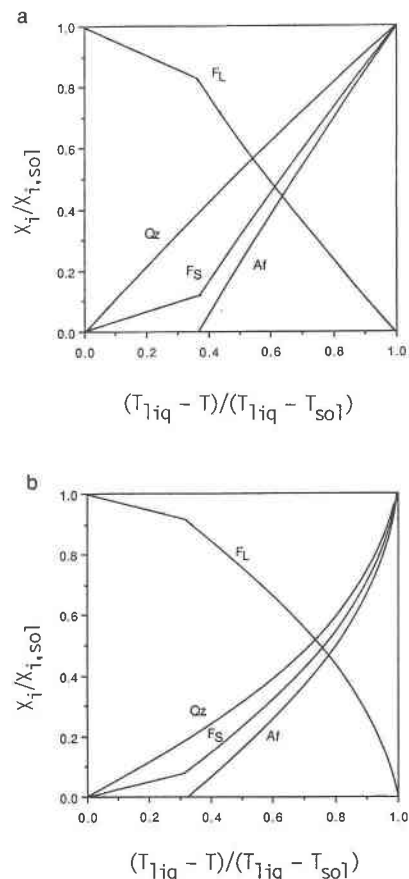


Fig. 4. Variation in modal proportions (X_i , on a mole fraction basis) of quartz, alkali feldspar, and quartz + alkali feldspar (F_s), relative to their proportions at the solidus ($X_{i,so}$), as a function of the fraction of the total crystallization temperature interval attained [i.e., $(T_{liquidus} - T)/(T_{liquidus} - T_{solidus})$]. Modal proportion of melt (F_L) is calculated relative to its proportion at the liquidus. (a) HG-1 at 2-kbar total pressure. (b) HG-1 at 5-kbar total pressure.

the tetrahedron (Fig. 6) are two major cotectic surfaces (plagioclase + quartz + liquid; plagioclase + alkali feldspar + liquid) and the minor alkali feldspar + quartz + liquid cotectic surface. These three surfaces intersect along a four-phase (or five-phase) curve that emanates from the ternary eutectic in the bounding ternary subsystem An-Or-Qz and extends toward the haplogranite (Ab-Or-Qz) thermal minimum. Most extensive within this system is the plagioclase + liquid field (or plagioclase + liquid + vapor field if H₂O-saturated); least extensive is the alkali feldspar + liquid (or alkali feldspar + liquid + vapor) field. The crystallization path followed by melts in the "granite" system is dependent upon the effects of pressure and H₂O content on the positions of the cotectic surfaces. Inasmuch as the effects of these variables on the cotectic surfaces were discussed in detail in Nekvasil and Burnham (1987), discussion here will focus on the effects of pressure and H₂O content on the four-phase surface (or five-phase curve if fluid-saturated) in the hydrous "granite" system.

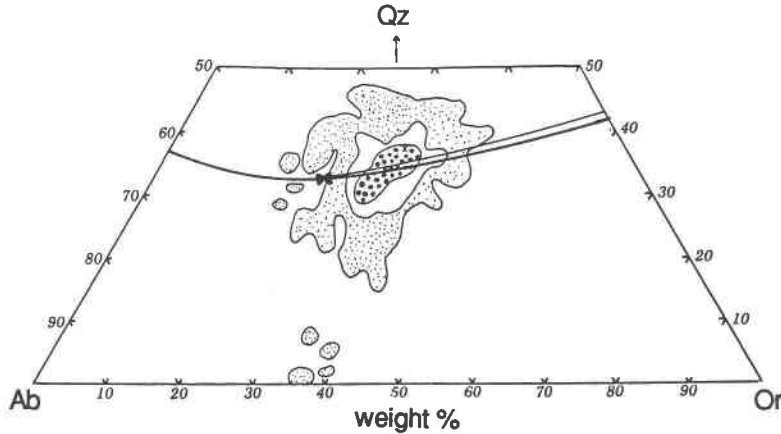


Fig. 5. Density contours depicting compositional frequency of occurrence of granites with normative $Ab + Or + Qz \geq 80$ wt% compiled by Washington (1917) (from Tuttle and Bowen, 1958). Superimposed for comparison is the H_2O -saturated 2-kbar haplogranite cotectic (heavy curve) and the H_2O -saturated 2-kbar four-phase curve projected from the An apex (thin curve). The projected composition of HG-1 is indicated by an \times (near top of highest-density area).

Early studies of An-bearing granitic compositions lying within the "granite" system that were directed toward understanding of the nature of the five-phase curve in P - T - X space included those of Winkler and von Platen (1960, 1961) and von Platen (1965). Winkler and von Platen (1960, 1961) melted calcite-bearing clays with different Na_2O contents as well as high-grade metagraywackes in the presence of excess water vapor at 2 kbar. They noted that the presence of the An component in the clays resulted in partial melts that lay (in projection) toward the Qz-Or side of the haplogranite minimum. They concluded that the higher the An content of the source material, the further toward this sideline the early-formed

melt would lie and the higher the solidus temperature would be. Therefore, the An/Ab ratio of the source region would strongly affect both the Or/Qz ratio of the melt as well as the melting temperature (which could vary by as much as 100 °C along the five-phase curve). The results of their vapor-present melting of metagraywackes indicated that most of the melting of such source materials occurs along the five-phase curve, the extent of melting along the curve being lower if the source rock contained high quantities of quartz and plagioclase.

Piwinskii and Wyllie (1968) looked at the melting relations of a granodiorite (the Needle Point pluton of the Wallowa batholith, Oregon). They found that the first liquid formed upon partial melting of granodiorite is composed largely of feldspars and quartz. Within 30 °C, nearly 50% of the rock was fused, and the Qz content of the melt increased very slowly within this melting interval. Although Johannes (1985) has suspected that their results are imprecise owing to the great probability of unstable melting of plagioclase in their experiments, their general trends are in keeping with those of earlier and later works.

Von Platen (1965) attempted a specific study of the five-phase curve at 2 kbar by locating the piercing points (which he called "eutectics") of this curve in the subsystems Pl-Qz-Or- H_2O , where Pl represents plagioclase components with variable An/Ab ratios. His results agreed with the earlier work of Winkler and von Platen (1960, 1961) in that they indicated the shift of the piercing points toward the Or-Qz sideline with increasing An content. He noted, however, that this shift was nonlinear with An content—the shift becoming increasingly smaller per increment change in An/Ab ratio at higher An content.

James and Hamilton (1969) determined phase relations in the "granite" system experimentally at 1 kbar (supplementing the data of von Platen, 1965, at 2 kbar) under H_2O -saturated conditions by looking at the piercing points of the five-phase curve as it sweeps from the

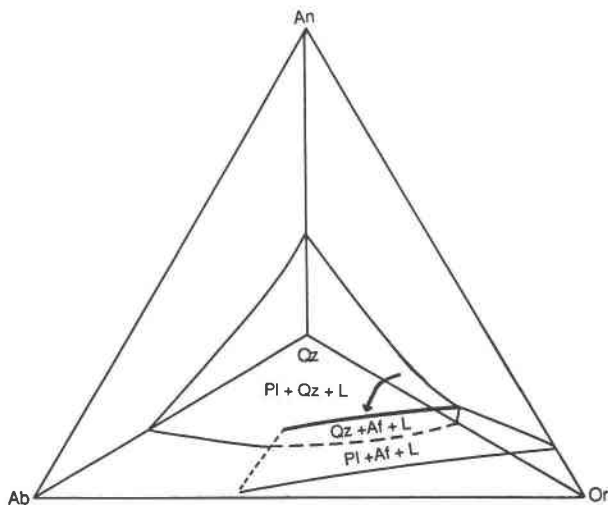


Fig. 6. Schematic diagram of the "granite" tetrahedron at constant H_2O content. The three cotectic surfaces plagioclase + quartz + liquid, plagioclase + alkali feldspar + liquid, and alkali feldspar + quartz + liquid are labeled. The four-phase (or five-phase) isobaric isoplethal curve (shown by arrow) marks the intersection of the three cotectic surfaces.

Ab-free system toward the haplogranite minimum. Although they could not determine melt compositions and could only partially analyze feldspars, their experimental data are useful for verifying the general trends obtained from the earlier work. Their recognition of these invariant points as piercing points and not as eutectics yielded the significant conclusion that once the liquid reached equilibrium with a vapor phase and three crystalline phases, it was still free to change composition with falling temperature. They were able to obtain the composition of the eutectic in the Ab-free system at $P_{H_2O} = 1$ kbar and found (as Yoder et al., 1957, had determined to be the case at 5 kbar) that the An content was very low (7.5–10 wt% An). Also important, James and Hamilton (1969) compared the concentration of compositions of granitic rocks from Washington's tables (1917) (as shown in Fig. 5) with the projected position of their piercing points. The higher Or/Ab ratios of the rocks relative to the haplogranite minimum supports an explanation of the displacement of the compositions as a result of the influence of An.

The five-phase curve has also been the object of intense experimental investigation by Winkler and Lindemann (1972), Winkler and Ghose (1973), and Winkler et al. (1975, 1977). Winkler and Lindemann (1972) investigated the effect of increasing P_{H_2O} on the composition of the ternary eutectic in the system Or-An-Qz-H₂O, which marks the emanation point of the five-phase curve. At 2-kbar P_{H_2O} , they located the eutectic at 9 and 14 wt% An for 2 and 5 kbar, respectively. When compared with the eutectic composition for the bounding H₂O-saturated system An-Or-H₂O, as determined by Yoder et al. (1957) at 5 kbar, these results imply that the cotectic (in the anhydrous projection of the system An-Or-Qz-H₂O), along which anorthite, K-feldspar, liquid, and vapor coexist, exhibits either no change in An content at 5-kbar P_{H_2O} or an increase in An content as it sweeps from the bounding subsystem An-Or-H₂O into the system An-Or-Qz-H₂O. If the An content of the melt did not decrease along the anorthite + K-feldspar cotectic upon the addition of Qz, the An in the melt must be experiencing strong negative deviations from ideality. In view of the data of Navrotsky et al. (1980) and the calculations of Burnham and Nekvasil (1986) and Nekvasil and Burnham (1987), it is not likely that such strong negative deviations from ideality are induced by the addition of Qz. In keeping with less extreme nonideal mixing behavior of the melt components in this system, the calculated eutectic in the system An-Or-Qz-H₂O lies at lower An contents than that of Winkler and Lindemann (1972).

Winkler and Lindemann (1972) concluded on the basis of their determinations of the position of the An-Qz-Or-H₂O eutectic at 2 and 5 kbar and those of Winkler and Ghose (1973) at 4 and 7 kbar that, in projection into the anhydrous system Qz-Or, there is little change in the eutectic composition with pressure, the major change occurring in the An content of the eutectic, which increased from 9 wt% at 2 kbar to 18 wt% at 5 kbar. However,

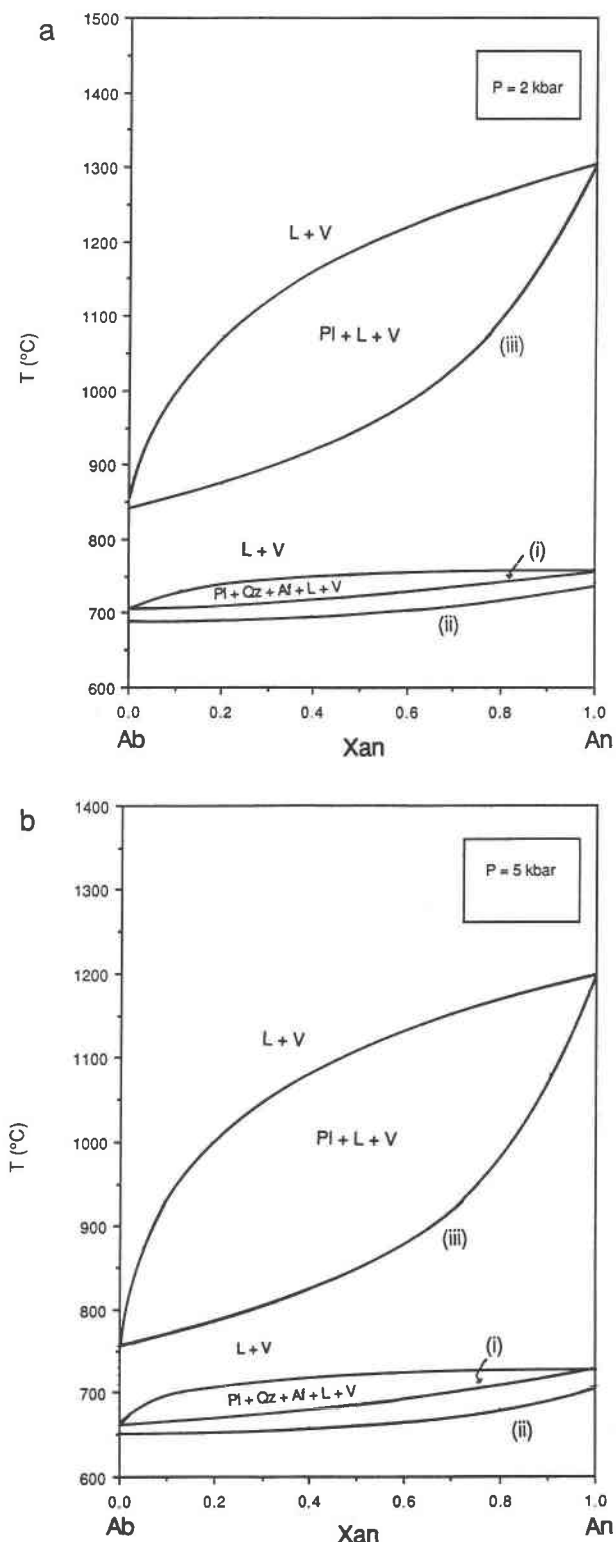


Fig. 7. The calculated (i) and experimentally determined (ii; from Johannes, 1980, 1984) five-phase solidus projected into the anhydrous system Ab-An at (a) $P_{H_2O} = 2$ kbar and (b) $P_{H_2O} = 5$ kbar. The calculated five-phase liquidus is also shown. For comparison, the plagioclase melting loops at 2 and 5 kbar from Nekvasil and Burnham (1987) (iii) are also indicated.

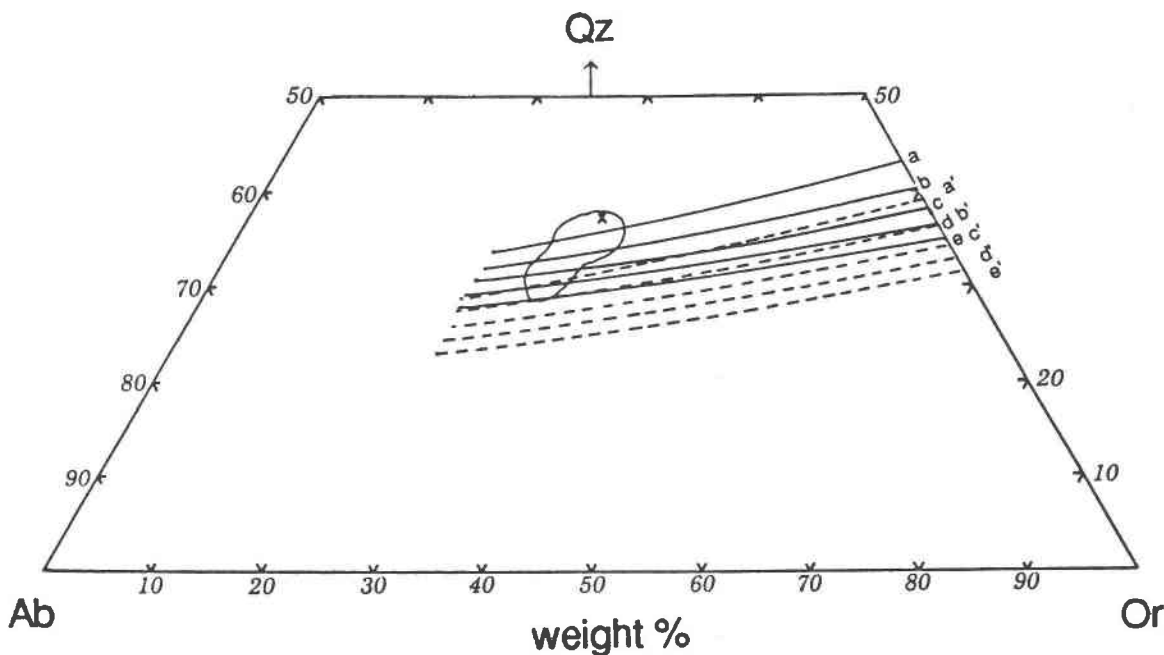


Fig. 8. Calculated four-phase surface in the system Ab-An-Or-Qz-H₂O at (a) 2 kbar (solid curves) and (b) 5 kbar (dashed curves) projected into the anhydrous haplogranite system as two sets of four-phase H₂O isoactivity curves. The two sets of isoactivity curves are labeled (a-e and a'-e') for each 0.2 increment of a_w (from 1.0 to 0.2) for 2 and 5 kbar, respectively. The highest compositional density contour of Figure 5 and the projected composition of HG-1 (x) are shown for reference.

owing to the smaller $\Delta H_{\text{fus}}^{\text{Si}_4\text{O}_8}$ and larger $\Delta V_{\text{fus}}^{\text{Si}_4\text{O}_8}$ relative to Or and An, it is unlikely that pressure would not affect the Or/Qz ratio.

Winkler et al. (1975, 1977) attempted to determine phase relations close to the five-phase curve at several pressures under H₂O-saturated conditions. At pressures below 7 kbar, they obtained a complicated configuration of the five-phase curve involving several pronounced inflections. At 7 kbar, however, they obtained a more linear relation. In light of his investigation of the equilibration rate of plagioclase as a function of temperature, Johannes (1978), however, concluded that the results of Winkler et al. (1975, 1977) were not equilibrium results but rather the results of metastable melting.

Johannes (1980, 1984) determined the solidus temperatures of source materials in equilibrium with plagioclase, alkali feldspar, and quartz at 2 and 5 kbar under H₂O-saturated conditions. Unlike the conclusions of Winkler et al. (1975, 1977), Johannes (1980, 1984) concluded that the solidus temperature of the five-phase curve increases very slowly with increasing An content. He obtained a total temperature change from the haplogranite minimum or eutectic to the eutectic in the Ab-free system of approximately 50 °C. In these experiments, however, he suggested that the actual melting temperatures may be as much as 10 °C higher than those that he obtained because of the possibility of metastable melting. The results of the solidus determinations of Johannes (1980, 1984) are shown in Figure 7. The calculated five-phase liquidus and solidus curves at 2 and 5 kbar under H₂O-saturated con-

ditions are also shown as projections into the anhydrous plagioclase system. At 5 kbar the melting loop extends to the haplogranite system. At 2 kbar, however, critical behavior is manifested, and the melting loop terminates slightly before the haplogranite system is reached. As was determined by Johannes (1984) for both 2- and 5-kbar $P_{\text{H}_2\text{O}}$, the calculated total temperature interval between the haplogranite thermal minimum and the An-Or-Qz eutectic is roughly 50 °C. Although the data of Johannes (1984) indicates that this temperature interval remains essentially constant with increasing $P_{\text{H}_2\text{O}}$, the calculated results indicate a slight increase in this temperature interval. The approximately 20 °C difference between the data of Johannes (1984) and the calculated solidi may be a result of a systematic error in the calculations or may be indicative of metastable melting.

Because of the difficulties in obtaining equilibrium assemblages in experimental investigations of the "granite" system, experimental data on the position of the four-phase (plagioclase + alkali feldspar + quartz + liquid) surface under H₂O-undersaturated conditions are not available. Instead, as was done for the cotectic surface in the system Ab-Or-Qz-H₂O, a series of four-phase H₂O isoactivity curves was calculated. When taken together and projected into the anhydrous haplogranite system, these isoactivity curves map out the four-phase surface in the system Ab-Or-An-Qz-H₂O. Figure 8 shows the projected surfaces at 2- and 5-kbar total pressure. The maximum An content along this surface (which is computed to lie at ≤ 6 wt% at these pressures) occurs at

the projected ternary eutectic in the system An-Or-Qz. The minimum An content along this surface is 0 wt% only if the four-phase surface extends to the haplogranite system. The effects of pressure and H₂O content on the four-phase H₂O isoactivity curves mirror those shown in Figure 1 for the cotectic isoactivity curves in the haplogranite system.

For several H₂O contents at 2- and 5-kbar pressure, the variation in temperature with position along the four-phase curves from the An-Or-Qz eutectic to the haplogranite minima is indicated in Figure 9a and 9b. This temperature variation is very slight [i.e., a temperature depression of generally less than 25 °C from an Ab/(An + Ab) molar ratio of 0 to 0.95 in the melt]. The magnitude of the temperature depression increases slightly with increasing H₂O content. These same characteristics are retained as total pressure is raised (cf. Figs. 9a, 9b). The Or content of the four-phase curve for a given Ab/(Ab + An) ratio decreases with increasing H₂O content as a reflection of the contraction of the quartz + liquid field with increasing H₂O content. As noted by von Platen (1965), at higher An contents there is a decrease in the extent of shift of the piercing points in the subsystems Pl-Qz-Or-H₂O toward the Or-Qz-H₂O sideline per incremental decrease in Ab/(Ab + An) ratio.

Beyond the readily apparent conclusion that the three crystalline phases plagioclase, alkali feldspar, and quartz can only coprecipitate in equilibrium with a melt at low An contents of the melt, several important characteristics of the four-phase surface have been brought to light in the above discussion. The slight temperature variation along the four-phase H₂O isoplethal curves indicates that along the four-phase surface, a small drop in temperature will produce a large change in melt composition and thereby a large increase in proportions of crystals (a phenomenon observed by Piwinski and Wyllie, 1968). Owing to the very small change in An content along the four-phase curve, the large amount of crystallization will affect the An content of the melt to only a small degree (but may produce large changes in plagioclase composition). Similarly, differences in the An content of a source region will produce only small changes in the solidus temperature and solidus melt composition. The nonlinear variation of Ab/(An + Ab) ratios along the calculated four-phase isopleths is in agreement with Winkler and von Platen (1960, 1961); however, the inflections obtained by Winkler et al. (1975, 1977) along the H₂O-saturated four-phase curves for pressures below 7 kbar were not detected through calculation. Such inflections, if real, would imply oscillations in activity coefficients of the feldspar components in the melt or crystalline phases.

The four-phase surface must be taken into account if H₂O is to be considered an independent compositional variable in the "granite" system. As was shown to be the case for equilibrium crystallization in the system Ab-Or-Qz-H₂O, the increase in H₂O content accompanying closed-system H₂O-undersaturated equilibrium crystallization will cause the melt to cut across the four-phase

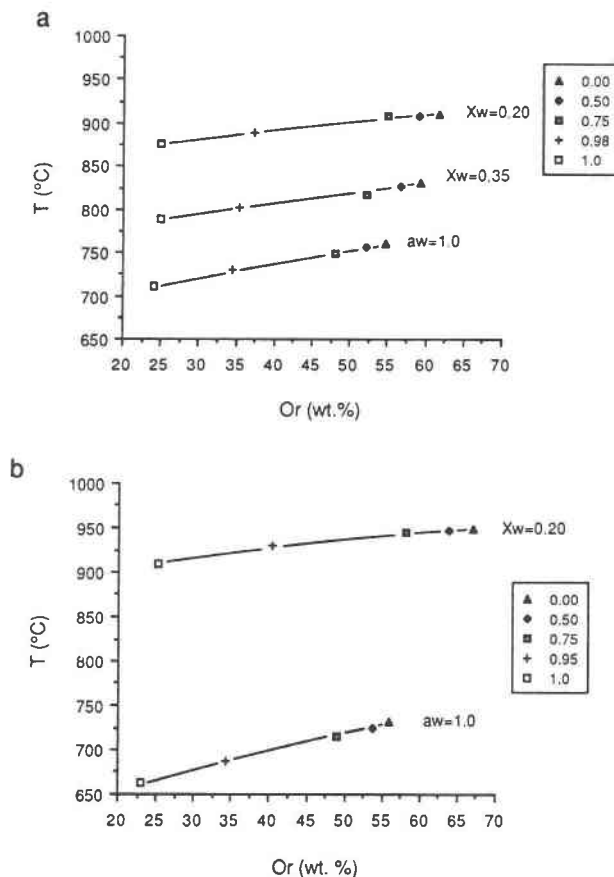


Fig. 9. Variation in temperature along (a) the $X_w = 0.20$, $X_w = 0.35$, and $a_w = 1.0$ four-phase (or five-phase) isoplethal and isoactivity curves at 2 kbar and (b) the $X_w = 0.20$ and $a_w = 1.0$ isoplethal and isoactivity curves at 5 kbar. Symbols represent the molar Ab/(Ab + An) ratios in the melt along the four-phase curves. Only the H₂O-saturated five-phase isoactivity curve at 5 kbar extends to the haplogranite system. The other isoactivity curves terminate in critical endpoints close to the haplogranite minima.

surface. Therefore, (1) the variation in temperature will be larger, (2) the variation in An content of the melt will be smaller, and (3) the change in percentage of crystals per unit change in $(T_{\text{liquidus}} - T)/(T_{\text{liquidus}} - T_{\text{solidus}})$ will be smaller than would be the case if the melt followed a single four-phase H₂O isoactivity curve. The compositions of the melts produced during crystallization will depend upon pressure: decreasing pressure at constant a_w or constant X_w will result in the production of more Qz-enriched daughter melts. At a constant total pressure, the position at which the crystallization paths will first intersect the four-phase surface will be very similar for melts with low Ab/(An + Ab) ratios but will differ more strongly for melts with high Ab/(An + Ab) ratios.

In order to compare crystallization paths in the granite tetrahedron relative to those in the haplogranite system, 5 mol% (5.4 wt%) and 10 mol% (10.7 wt%) An component was added to the composition HG-1 to obtain the

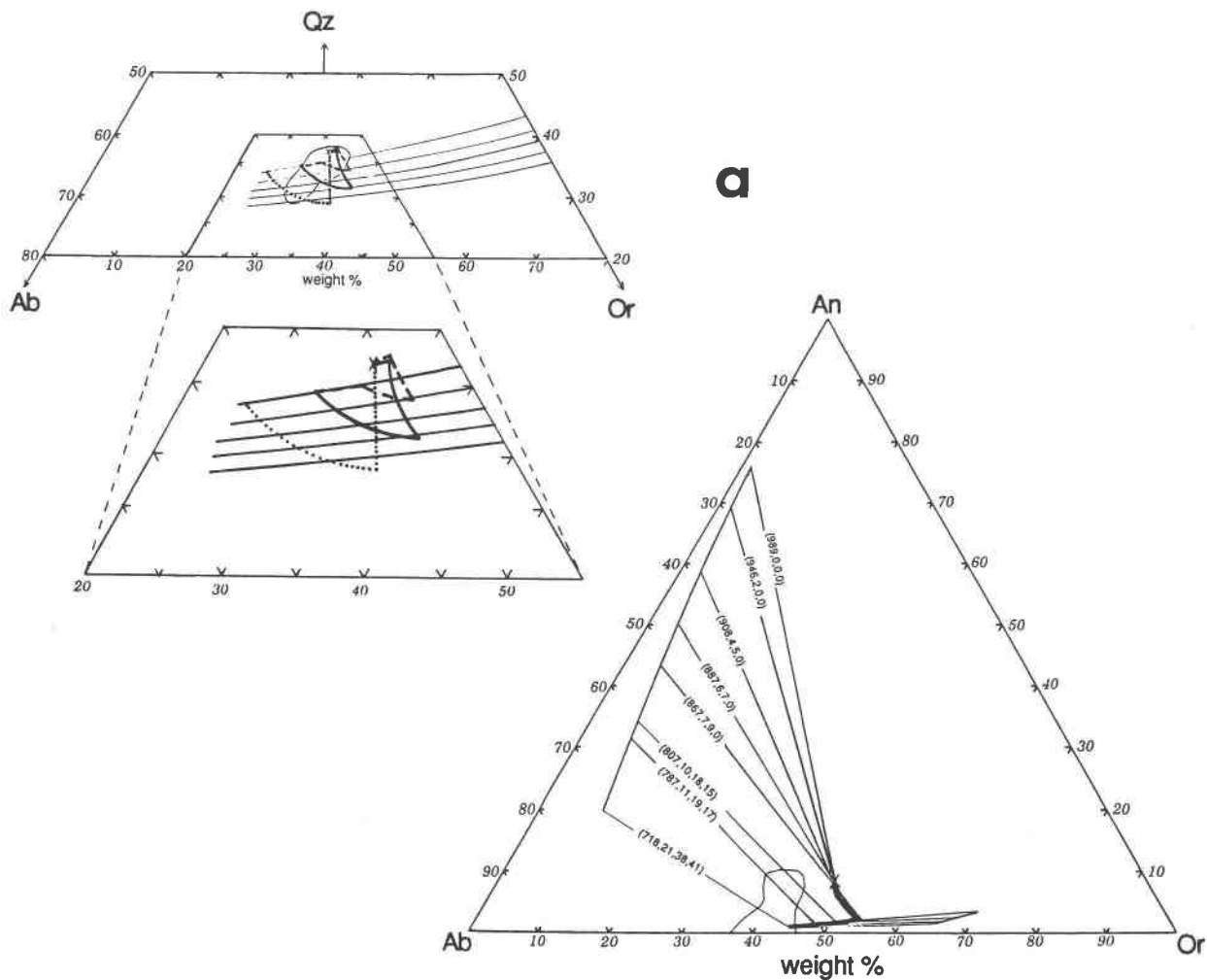
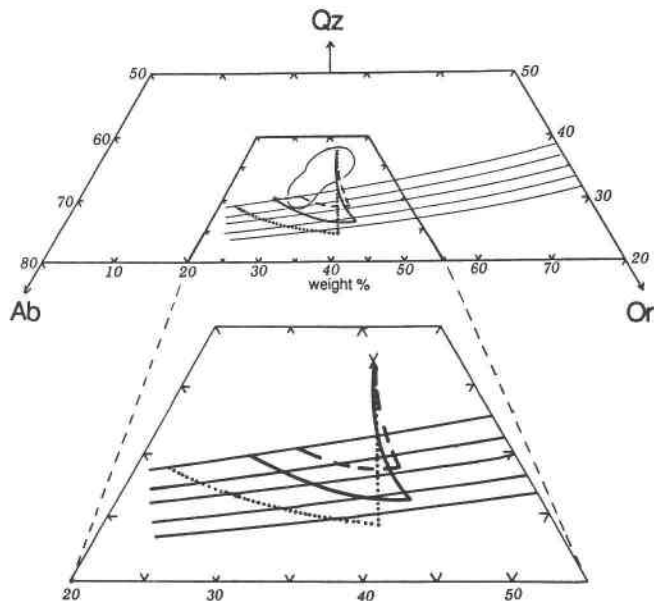
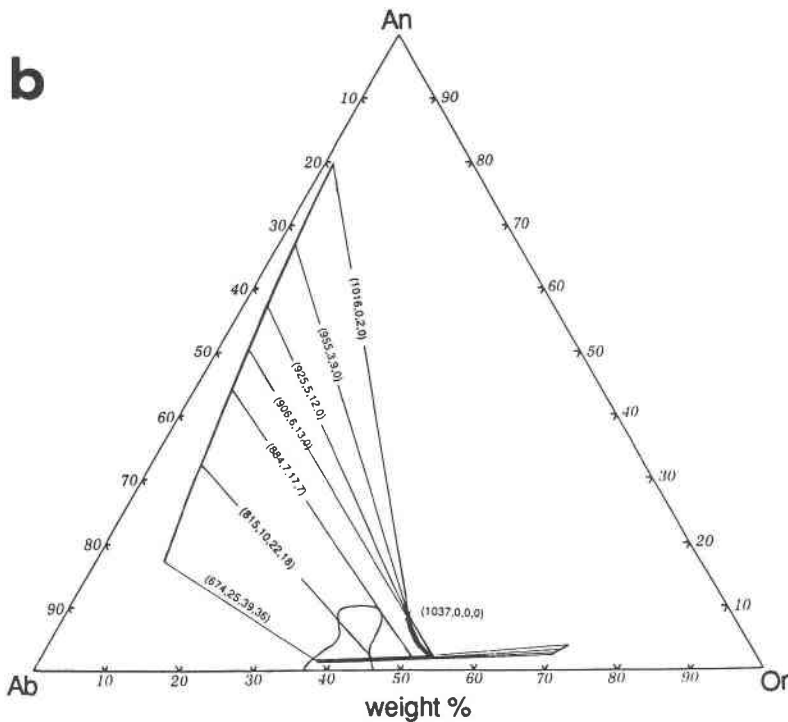
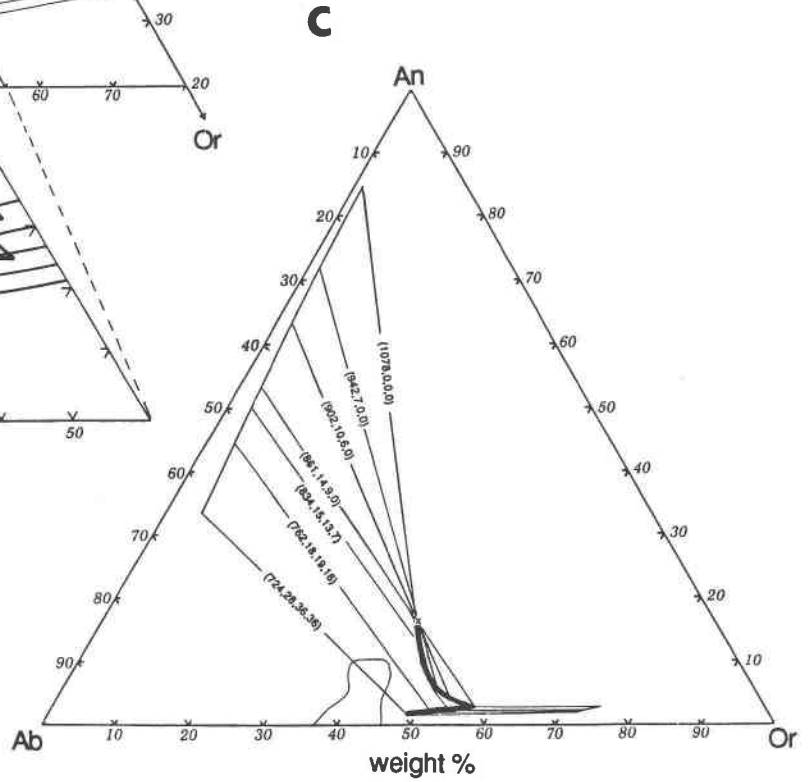
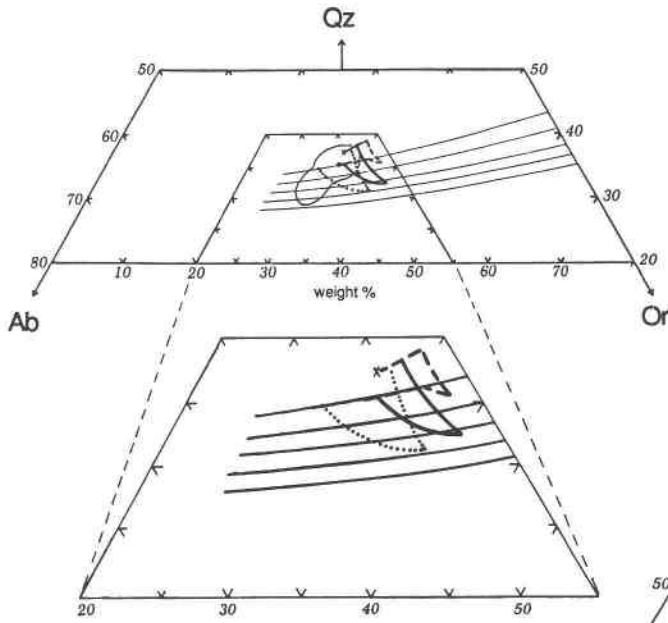


Fig. 10. Calculated crystallization path of HGAn-1 (HG-1 + 5 mol% An). Three pairs of projections showing calculated crystallization paths: (a) HGAn-1 (HG-1 + 5 mol% An) at 2-kbar total pressure, (b) HGAn-1 at 5-kbar total pressure, and (c) HGAn-2 (HG-1 + 10 mol% An) at 2-kbar total pressure. \times symbols indicate projected position of bulk composition. The highest-density contour of the frequency of occurrence of natural compositions with normative Ab + Or + Qz > 80% (from Tuttle and Bowen, 1958, and James and Hamilton, 1969) is shown in both the haplogranite (left-hand part of each pair) and feldspar (right-hand part) projections.

In left-hand part of each pair, paths for the bulk compositions including 1.7 wt% H₂O (heavy solid curves) and 3.5 wt% H₂O





(dashed curves) are projected into haplo-granite system. Dotted curves show crystallization paths for (a and b) the An-free composition (HG-1) with 1.7 wt% H₂O and (c) the 5 mol% An composition (HGAn-1) with 1.7 wt% H₂O. The set of four-phase isoactivity curves from Fig. 8 are also plotted for comparison.

In right-hand part of each pair, paths for the bulk composition including 1.7 wt% H₂O are projected into feldspar system. Tie lines indicate compositions of coexisting feldspars and melt; temperature and relative amounts of plagioclase, quartz, and alkali feldspar (mol%) in system are indicated sequentially in parentheses along each tie line. Light curves indicate a polythermal section of feldspar solvus.

compositions HGAN-1 and HGAN-2, respectively. In projection onto the haplogranite base, these compositions will be coincident with HG-1. Figure 10a shows the calculated crystallization path of HGAN-1 for 20 and 35 mol% H₂O (~1.7 and ~3.7 wt% H₂O) at 2-kbar total pressure projected onto the anhydrous haplogranite base. The crystallization path of HG-1 is also shown for comparison. The addition of 5 mol% An stabilizes plagioclase as the liquidus phase, which is followed by quartz crystallization and finally by alkali feldspar. At 2 kbar, a melt of HGAN-1 composition (with bulk H₂O content of 1.7 wt%) first moves away from the Ab-An sideline upon the precipitation of plagioclase of An₇₆Ab₂₃Or₁ composition at 989 °C. Very soon, however, quartz begins to coprecipitate with plagioclase, and the melt becomes enriched in Or component. Alkali feldspar (of Or₆₉Ab₂₈An₃ composition) appears when the melt reaches the four-phase surface at the four-phase isoplethal curve for which $X_w = 0.239$; by this point (867 °C) the plagioclase composition has shifted to An₄₁Ab₅₃Or₆. Continued crystallization results in the enrichment of the melt in Ab and Qz as the melt path cuts across the four-phase surface toward the H₂O-saturated five-phase curve and then to the solidus. As with haplogranitic melts, the main deviation of this path from the H₂O-saturated crystallization paths is the Qz enrichment of the melt, which occurs as the melt cuts across the four-phase surface. Whitney (1969) was able to obtain valuable, although limited, compositional data on H₂O-undersaturated melting paths in the "granite" system. His experimental results indicate the same trends as those calculated. He determined that the effect of adding An component to a haplogranitic melt is a displacement of the projected crystallization path toward the Or-Qz sideline. He was also able to document the Qz depletion in melts that occurs during melting as the melt path cuts across the four-phase surface.

As the bulk H₂O content increases (e.g., from 1.7 to 3.7 wt% H₂O), the melt will reach the five-phase H₂O-saturated isoactivity curve at an earlier stage of crystallization, and further crystallization will induce a slight Qz depletion of the late-stage melt. It is apparent that the addition of An to haplogranitic melts induces a contraction of the compositional range (in projection) of possible daughter melts produced by differentiation and induces an apparent enrichment of Or and Qz components in the melts produced along the crystallization path.

The precipitous drop in An content of the melt during the early stages of crystallization is shown in Figure 10a by the projection of the crystallization path of HGAN-1 (1.7 wt% H₂O) into the anhydrous feldspar system (i.e., the system Ab-An-Or) at 2-kbar total pressure. The very steep drop in An content of the melt is only slightly affected by the onset of precipitation of quartz and continues until alkali feldspar is stabilized. The variation in An content in the melt from this point on to the solidus is very slight, although of the original quantity of melt, 84 mol% still remains to crystallize.

As the pressure increases to 5 kbar, the compositional

space over which crystallization takes place expands (Fig. 10b) as was the case for HG-1. The increase in Or content of the daughter melts produced by the composition HGAN-1 is evident, as is the change of the melt composition at the solidus to a more Or-rich composition. Because of the shift of the four-phase H₂O isoplethal or isoactivity curves to lower Qz contents with increasing pressure, derivative melts generated by differentiation will be lower in Qz at 5 kbar than at 2 kbar. Figure 10b also shows the crystallization path of HGAN-1 at 5 kbar projected into the anhydrous feldspar system. Although the composition of the earliest-formed plagioclase is more An rich at 5 kbar than at 2 kbar, alkali feldspar appears at approximately the same projected melt composition at both pressures. Inasmuch as the solubility of H₂O in the melt increases with pressure, the melt intersects the four-phase surface at a lower H₂O isoactivity curve at 5 kbar and must therefore travel a greater distance across the surface before reaching the H₂O-saturated isoactivity curve. Accordingly, the plagioclase composition starts at a higher An content and reaches a lower An content at the solidus than would be the case at lower pressure.

The effect of increasing the An content of the bulk composition to 10 mol% at 2-kbar total pressure is shown in Figure 10c. The Or enrichment seen in Figures 10a and 10b is magnified for this composition, and the entire projected crystallization path is shifted even further toward the Qz-Or sideline as the increase in An content further stabilizes plagioclase. This shift, however, is not quite as strong as was the case for the addition of the first 5 mol% An to HG-1. Interestingly, A.J.R. White (pers. comm.) noted that the average plagioclase cores in granitoids are of An₈₀ composition. Additionally, the solidus plagioclase composition and phase proportions (Fig. 10c) are typical of granodiorites.

Figure 11a shows the variation in the proportions of phases with incremental increase of $(T_{\text{liquidus}} - T)/(T_{\text{liquidus}} - T_{\text{solidus}})$ for HGAN-1 at 2 kbar and bulk H₂O content of 1.7 wt%. The basic characteristics of this variation are very similar to that for HG-1. For a bulk H₂O content of 1.7 wt%, 30 mol% of the system crystallizes in the first 50% of the crystallization temperature interval. A similar diagram for bulk H₂O content of 3.5 wt% is shown in Figure 11b. It is apparent that the effect of increasing H₂O is to strongly depress crystallization during the early stages of crystallization. [This effect had been noticed by Steiner et al. (1975) during their experimental investigation of crystallization of H₂O-undersaturated haplogranitic melts.] In the first 50% of the temperature interval, only 5% of the melt has crystallized; yet by this stage, the plagioclase composition has changed from An₇₈Ab₂₁Or₁ to An₅₅Ab₄₂Or₂. The variation in modal abundances at 5-kbar total pressure is shown in Figure 11c. The activity of H₂O represented by the initial 1.7 wt% H₂O is now smaller than at 2 kbar and results in the strongly nonlinear variation in proportions of crystalline material with incremental increases in $(T_{\text{liquidus}} - T)/(T_{\text{liquidus}} - T_{\text{solidus}})$. Figure 11d shows for comparison the variation in modal abun-

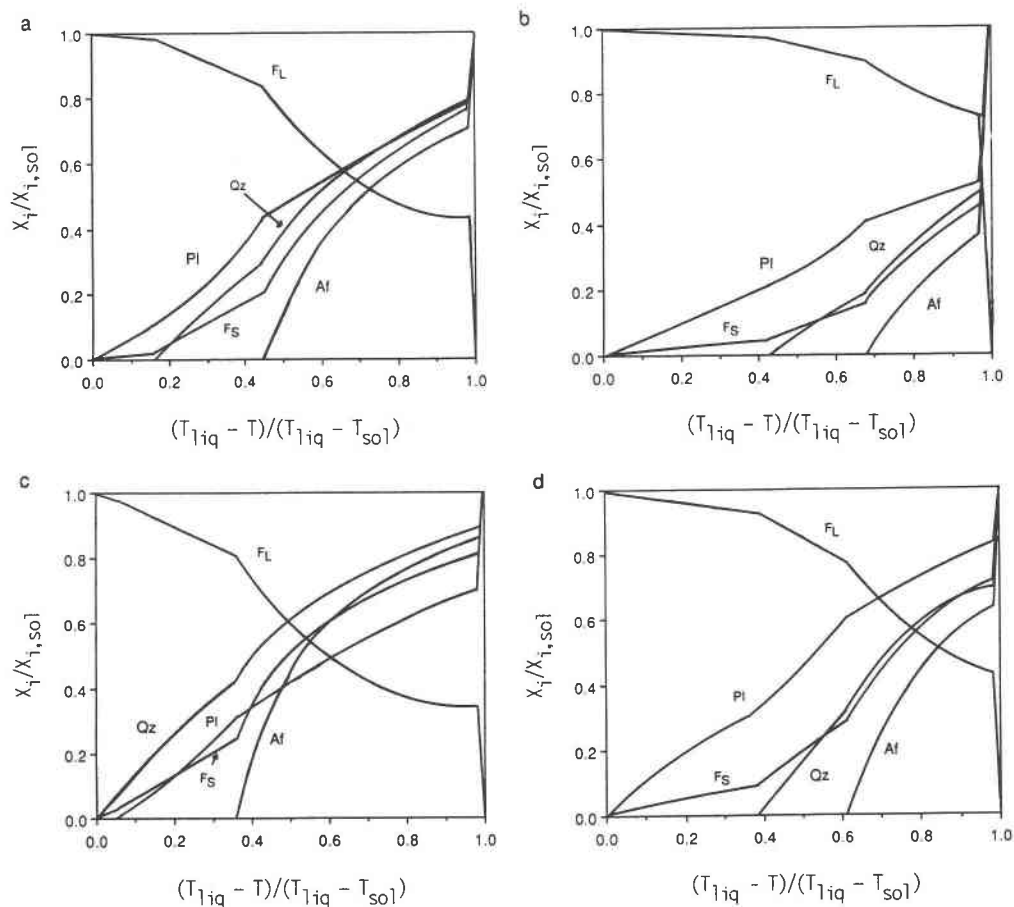


Fig. 11. Variation in modal proportions (X_i , on a mole fraction basis) of plagioclase, alkali feldspar, quartz, and all crystalline phases (F_s) relative to their proportions at the solidus ($X_{i,so}$) as a function of the fraction of the total crystallization temperature interval attained [i.e., $(T_{\text{liquidus}} - T)/(T_{\text{liquidus}} - T_{\text{solidus}})$]. Modal proportion of melt (F_L) is calculated relative to its proportion at the liquidus. (a) HGAn-1 at 2 kbar; bulk H_2O content, 1.7 wt%; (b) HGAn-1 at 2 kbar; bulk H_2O content, 3.5 wt%; (c) HGAn-1 at 5 kbar; bulk H_2O content, 1.7 wt%; and (d) HGAn-2 at 2 kbar; bulk H_2O content, 1.7 wt%.

dances for HGAn-2 at 2 kbar. The increase in An content of the bulk composition results in early stabilization of plagioclase and thus a greater extent of plagioclase precipitation before quartz and alkali feldspar appear. The general morphology of the variation curves, however, remains the same.

CONCLUSIONS

The crystallization paths in the haplogranite system as determined by the H_2O -saturated phase relations of Tuttle and Bowen (1958) and Luth et al. (1964) are significantly modified under hydrous but H_2O -undersaturated and unbuffered conditions. Under such conditions the cotectic curve in the haplogranite system becomes a cotectic surface that can be described by a series of cotectic H_2O isoactivity curves. These isoactivity curves shift toward the Qz apex with increasing H_2O content and away from the Qz apex with increasing pressure. Closed-system crystallization paths of H_2O -undersaturated haplogranitic melts will show continuous Qz enrichment of the melt instead of depletion during the coprecipitation of quartz

and alkali feldspar until the H_2O -saturated ($a_w = 1$) cotectic isoactivity curve is reached. The range of melt compositions that can be generated by differentiation is greater at high pressures owing to the shift of the cotectic surface away from Qz. Higher-pressure differentiates and partial melts will, therefore, be lower in Qz than if they had formed at lower pressure. With increased H_2O contents, the increasing nonlinearity of the variation of modal percentages of precipitated phases with increasing $(T_{\text{liquidus}} - T)/(T_{\text{liquidus}} - T_{\text{solidus}})$ indicates that partial melts derived from source regions with relatively high H_2O contents should cluster around the haplogranite minimum composition unless the An content of the source region is high.

Tuttle and Bowen's (1958) summary of compositions of granites with normative $\text{Ab} + \text{Or} + \text{Qz} \geq 80\%$ indicates a strong displacement away from the haplogranite minima toward the Or-Qz sideline in the direction of the four-phase surface in the system Ab-Or-An-Qz- H_2O . Calculations of equilibrium crystallization paths indicate that the result of adding An to haplogranitic compositions is

the shift of each entire crystallization path (as well as the solidus) toward the Or-Qz sideline. For high H₂O contents, the increased extent of crystallization near the solidus indicates that for any reasonable amount of partial melting (e.g., 25–40%) of a plagioclase-bearing, H₂O-rich source, the resulting melt will lie along the four-phase surface and hence be multiply saturated in plagioclase, alkali feldspar, and quartz. The nonlinear increase of the Ab/(Ab + An) molar ratio of the melt along the four-phase isoactivity curves indicates that most such melts, even those produced in source regions with relatively high An content, will lie clustered in the Ab-rich region of the four-phase surface and will therefore have low An contents. Inasmuch as a large extent of melting could take place under H₂O-saturated conditions without much change in temperature, the liquidus temperatures of such magmas will be low. Additionally, a series of granites produced by partial melting of such an H₂O-rich source region would have relatively invariant Qz contents and differ mainly in Ab/Or ratio. If on the other hand, the H₂O content of the source region were low, then it is likely that partial melting to the extent of 25–40% will produce melts off of the four-phase surface and very likely in the plagioclase field.

It was the intent of this article to stimulate thought regarding the individual effects of H₂O, total pressure, and An content on crystallization paths of “granitic” compositions. Until more experimental data are available for comparison, the accuracy of the predicted saturation temperatures presented here cannot be fully evaluated. However, the trends shown are thermodynamically reasonable and as such are invaluable in predicting the trends in compositional variation of a series of daughter melts related by differentiation or equilibrium melting. The compositions evaluated in this article are those that characterize common natural compositions. Other more unusual (e.g., very albitic) compositions may show considerable deviations from the crystallization paths discussed above. At low P_{H_2O} , the four-phase surface does not extend to the haplogranite system, and critical behavior is manifested. For albitic, Qz-poor compositions, coprecipitation of two feldspars may be replaced by a reaction relation between plagioclase and melt [as seen for very albitic compositions along the cotectic in the system Ab-An-Or (Carmichael, 1963)]. The differentiation paths of the compositions discussed in this article did not enter such a region. However, in order to be able to quantitatively assess the nature of crystallization paths of natural low-An felsic melts, the effects of P , a_w , and a_{Qz} on the location and character of the “peritectic-like” regions must be evaluated and will be addressed in a later article.

ACKNOWLEDGMENTS

This work was supported in part by the National Science Foundation grants EAR 82-12492 awarded to C. Wayne Burnham and EAR 86-17128 to J. R. Holloway, which are gratefully acknowledged. The helpful reviews of J. Longhi, R. Luth, J. Holloway, and C. Wayne Burnham were greatly appreciated and resulted in numerous improvements to the manuscript.

REFERENCES CITED

- Burnham, C. Wayne. (1975) Thermodynamics of melting in experimental silicate-volatile systems. *Geochimica et Cosmochimica Acta*, 39, 1077–1084.
- (1981) Nature of multicomponent aluminosilicate melts. In D.T. Rickard and F.E. Wickman, Eds., *Chemistry and geochemistry of solutions at high temperatures and pressures. Physics and chemistry of the earth*, 13–14, 197–229.
- Burnham, C. Wayne, and Nekvasil, H. (1986) Granite pegmatite magmas. *American Mineralogist*, 71, 239–264.
- Carmichael, I.S.E. (1963) The crystallization of feldspar in volcanic acid liquids. *Quarterly Journal of the Royal Society of London*, 119, 95–131.
- Hervig, R.L., and Navrotsky, A. (1984) Thermochemical study of glasses in the system NaAlSi₃O₈-KAlSi₃O₈-Si₂O₆ and the join Na_{1.6}Al_{1.6}Si_{2.4}O₈-K_{1.6}Al_{1.6}Si_{2.4}O₈. *Geochimica et Cosmochimica Acta*, 48, 513–522.
- James, R.S., and Hamilton, D.L. (1969) Phase relations in the system NaAlSi₃O₈-KAlSi₃O₈-CaAl₂Si₂O₈-SiO₂ at 1 kilobar vapour pressure. *Contributions to Mineralogy and Petrology*, 21, 111–141.
- Johannes, W. (1978) The melting of plagioclase in the system Ab-An-H₂O and Qz-Ab-An-H₂O at $P(H_2O) = 5$ kbar: An equilibrium problem. *Contributions to Mineralogy and Petrology*, 66, 295–303.
- (1980) Melting and subsolidus reactions in the system K₂O-CaO-Al₂O₃-SiO₂-H₂O. *Contributions to Mineralogy and Petrology*, 74, 29–34.
- (1984) Beginning of melting in the “granite” system Qz-Or-Ab-An-H₂O. *Contributions to Mineralogy and Petrology*, 86, 264–273.
- (1985) The significance of experimental studies for the formation of migmatites. In J.R. Ashworth, Ed., *Migmatites*, p. 36–85. Chapman and Hall, New York.
- Luth, W.C. (1969) The systems Ab-Qz, Sa-Qz to 20 kbar and the relationship between H₂O content, P_{H_2O} and P_T in granitic magmas. *American Journal of Science*, 237A, 325–341.
- Luth, W.C., Jahns, R.H., and Tuttle, O.F. (1964) The “granite” system at 4 to 10 kbar. *Journal of Geophysical Research*, 64, 759–773.
- Navrotsky, A., Hon, R., Weill, D.F., and Henry, D.J. (1980) Thermochemistry of glasses and liquids in the system CaMgSi₂O₆-CaAl₂Si₂O₈-NaAlSi₃O₈, SiO₂-CaAlSi₃O₈-NaAlSi₃O₈ and SiO₂-Al₂O₃-CaO-Na₂O. *Geochimica et Cosmochimica Acta*, 44, 1409–1423.
- Nekvasil, H. (1986) A theoretical thermodynamic investigation of the system Ab-Or-An-Qz-H₂O and implications for melt speciation. Ph.D. dissertation, The Pennsylvania State University, State College, Pennsylvania.
- (1988) Calculation of equilibrium crystallization paths of compositionally simple hydrous felsic melts. *American Mineralogist*, 73, 956–965.
- Nekvasil, H., and Burnham, C. Wayne (1987) The individual effects of pressure and water content on phase equilibria in the “granite” system. In *Magmatic processes: Physicochemical principles*. Geochemical Society Special Publication 1, 433–445.
- Piwinskii, A.J., and Wyllie, P.J. (1968) Experimental studies of igneous rock series: A zoned pluton in the Wallowa batholith, Oregon. *Journal of Geology*, 76, 205–234.
- Platen, von H. (1965) Kristallisation granitischer Schmelzen. *Beiträge der Mineralogie und Petrologie*, 11, 334–381.
- Silver, L., and Stolper, E. (1985) A thermodynamic model for hydrous silicate melts. *Journal of Geology*, 93, 161–178.
- Steiner, J.C., Jahns, R.H., and Luth, W.C. (1975) Crystallization of alkali feldspar and quartz in the haplogranite system, NaAlSi₃O₈-KAlSi₃O₈-SiO₂-H₂O at 4 kbar. *Geological Society of America Bulletin*, 86, 83–98.
- Tuttle, O.F., and Bowen, N.L. (1958) Origin of granite in light of experimental studies in the system NaAlSi₃O₈-KAlSi₃O₈-SiO₂-H₂O. *Geological Society of America Memoir* 74, 145 p.
- Washington, H.S. (1917) Chemical analyses of igneous rocks. United States Geological Survey Professional Paper 99, 1201 p.
- Whitney, J.A. (1969) Partial melting relationships of three granitic rocks. M.S. dissertation, Massachusetts Institute of Technology, Cambridge, Massachusetts.
- Winkler, H.G.F., and Ghose, N.C. (1973) Further data on the eutectics

- in the system Qz-Or-An-H₂O. *Neues Jahrbuch der Mineralogie, Monatshefte*, 481-484.
- Winkler, H.G.F., and Lindemann, W. (1972) The system Qz-Or-An-H₂O within the granite system Qz-Or-Ab-An-H₂O. Application to granitic magma formation. *Neues Jahrbuch der Mineralogie, Monatshefte*, 49-61.
- Winkler, H.G.F., and Platen, von H. (1960) Experimentelle Gesteinsmetamorphose III. Anatektische Ultrametamorphose kalhaltiger Tone. *Geochimica et Cosmochimica Acta*, 18, 294-316.
- (1961) Experimentelle Gesteinsmetamorphose IV. Bildung anatektischer Schmelzen aus metamorphisierten Grauwacken. *Geochimica et Cosmochimica Acta*, 24, 48-69.
- Winkler, H.G.F., Boese, M., and Marcopoulos, T. (1975) Low temperature granitic melts. *Neues Jahrbuch der Mineralogie, Monatshefte*, 245-268.
- Winkler, H.G.F., Das, B.K., and Breitbarth, R. (1977) Further data of low temperature melts existing on the quartz + plagioclase + L + V isobaric cotectic surface within the system Qz-Ab-Or-An-H₂O. *Neues Jahrbuch der Mineralogie, Monatshefte*, 241-247.
- Yoder, H.S., Jr., Stewart, D.B., and Smith, J.R. (1957) Ternary feldspars. *Carnegie Institute of Washington Yearbook* 56, 206-214.

MANUSCRIPT RECEIVED OCTOBER 23, 1987

MANUSCRIPT ACCEPTED MAY 20, 1988